Nucleophilic Cleavage of Phosphate Triesters in Dialkylammonium Bilayer Membranes[1)]

Yoshio Okahata, Hirotaka Ihara, and Toyoki Kunitake*

Department of Organic Synthesis, Faculty of Engineering, Kyushu University, Higashi-ku, Fukuoka 812

(Received October 27, 1980)

A study was carried out on the reaction of *p*-nitrophenyl phosphates with hydroxamate nucleophiles in water in the presence of dialkylammonium bilayer membranes. With ethyl bis(*p*-nitrophenyl) phosphate, clean second-order kinetics was observed for all the hydroxamate nucleophiles, two equivalents of *p*-nitrophenol being released in most cases. In contrast, a complex kinetics was observed for octadecylbis(*p*-nitrophenyl)phosphate. The second cleavage process of this long-chain substrate by a long-chain hydroxamate was affected by the fluidity of the matrix membrane, an inflection region being present in the Arrhenius plots near the phase transition temperature(T_c) of the $2C_{16}N^+2C_1$ membrane. The activation energy was 14 and 21 kcal/mol at temperatures above and below T_c, respectively. Similar changes in the activation energy had been observed for decarboxylation and proton abstraction.

Since it was first found that bilayer membranes are formed from dialkylammonium salts,[2,3)] physicochemical characterization of the dialkylammonium bilayer has been extensively carried out. One important characteristic is the occurrence of the crystal-to-liquid crystal phase transition similar to that of biolipid bilayers, as confirmed by differential scanning calorimetry,[4,5)] NMR spectroscopy,[6)] fluorescence depolarization,[6,7)] and positron annihilation.[7)]

The unique organization of the dialkylammonium bilayer was subsequently used as site for several kinds of organic reaction. A large rate difference was observed between the intra-vesicle and inter-vesicle reactions of nucleophiles and a phenyl ester.[8)] A cholesteryl nucleophile was specifically activated in the ammonium membrane,[9)] and the reaction rate was influenced by the phase transition in acyl transfer,[10)] proton abstraction,[11)] and decarboxylation.[12)]

In this article we report on the hydrolysis of activated phosphoric triesters by hydrophobic hydroxamate nucleophiles in the presence of hexadecyltrimethylammonium bromide (CTAB) micelle and dialkylammonium ($2C_nN^+2C_1$) bilayer membranes.[13)] The hydrolysis of phosphoric triesters proceeds *via* general-base or nucleophilic pathways. The relative ease of these pathways is determined by structural combinations of substrates and bases, the relative basicity of leaving group and nucleophile and steric crowding in the transition state being concluded to be the two most important factors.[14—16)]

The micellar effect on the cleavage of phosphoric triesters was studied by Bunton and Ihara[17)] and Epstein *et al.*[18)] for oximate nucleophiles and by Tagaki *et al.*[19)] for imidazole nucleophiles. It was found that cationic micelles accelerate the reaction and change the mechanism. It is of particular interest to see how the peculiar molecular organization of the bilayer membrane affects the cleavage of phosphoric esters.

The structures of nucleophiles, substrates and membrane-forming ammonium salts used in this study are given below together with their abbreviations.

Ammonium salt

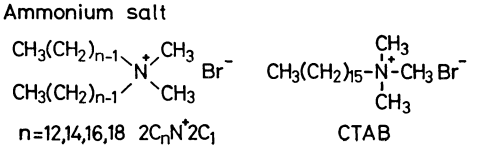

Nucleophile

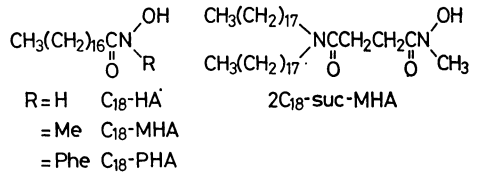

Substrate

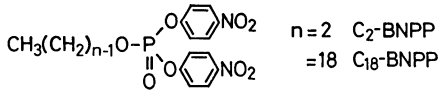

Experimental

Nucleophiles. Octadecanehydroxamic acid (C_{18}-HA), *N*-methyloctadecanehydroxamic acid (C_{18}-MHA), and *N*-phenyloctadecanehydroxamic acid (C_{18}-PHA) were prepared from octadecanoyl chloride and the corresponding hydroxylamines, and identified by NMR and IR spectroscopy and elemental analysis. C_{18}-HA: mp 102—104 °C. Found: C, 71.86; H, 12.46; N, 4.65%. Calcd for $C_{18}H_{37}NO_2$: C, 72.19; H, 12.45; N, 4.68%. C_{18}-MHA: mp 60—62 °C. Found: C, 72.59; H, 12.39; N, 4.40%. Calcd for $C_{19}H_{37}NO_2$: C, 72.79; H, 12.54; N, 4.47%. C_{18}-PHA: mp 88—89 °C. Found: C, 76.33; H, 10.97; N, 3.70%. Calcd for $C_{24}H_{41}NO_2$: C, 76.74; H, 11.00; N, 3.73%.

Mono-*N,N*-dioctadecylamide of succinic acid (9.3 g, 15 mmol) as prepared from dioctadecylamine and succinic anhydride, and 2 g (18 mmol) of *N*-hydroxysuccinimide were dissolved in 70 ml of tetrahydrofuran (THF), 3.7 g (18 mmol) of dicyclohexylcarbodiimide being added with stirring at ice-bath temperature. The reaction mixture was warmed to room temperature after 1 h and stirred for 24 h. *N,N'*-Dicyclohexylurea was filtered. After the solvent had been removed, the residue was recrystallized from 1:10 ether–methanol to give colorless powder: yield 9.3 g (86%), mp 64—67 °C. The succinimide ester obtained (5 g, 8 mmol) was dissolved in 30 ml of $CHCl_3$, and 2.5 g (30 mmol) of *N*-methylhydroxylamine and 3 g (30 mmol) of triethylamine in 60 ml of $CHCl_3$ were slowly added with stirring. After the mixture had been stirred for 6 h at room temperature, the solvents were evaporated and the residue was dissolved in ether, washed with dilute hydrochloric acid and water, and dried over Na_2SO_4. The solution was concentrated and 3 g of solids was recovered by addition of methanol. Colorless powder was obtained by repeated recrystalliza-

tion from 1:1 acetone–ether: yield 1.4 g (30%), mp 50—52 °C. The product, *N*-methyl-3-(dioctadecylcarbamoyl)propanehydroxamic acid, ($2C_{18}$-suc-MHA) was confirmed by IR and NMR spectroscopy and by elemental analysis. Found: C, 75.62; H, 12.80; N, 4.20%. Calcd for $C_{41}H_{82}N_2O_3$: C, 75.63; H, 12.69; N, 4.30%.

Preparation and purification of *N*-dodecylbenzohydroxamic acid (C_{12}-BHA),[20] and *N*-benzylbenzohydroxamic acid (BBHA)[21] were reported. $C_{12}N^+C_2$-MHA was supplied by T. Sakamoto.[22]

Substrates. Tris(*p*-nitrophenyl) phosphate (1 g, 2.2 mmol) was refluxed for 1 d in 10 ml of dry ethanol, coloreless needles of C_2-BNPP being obtained on cooling: yield 0.7 g (90%), mp 134—135 °C (lit,[23] mp 133 °C). The purity was confirmed by NMR spectroscopy and elemental analysis. Found: C, 45.50; H, 3.57; N, 7.68%. Calcd for $C_{14}H_{13}N_2O_8P$: C, 45.67; H, 3.56; N, 7.61%.

Triethylamine (3.7 g, 37 mmol) and 10.0 g (37 mmol) of octadecyl alcohol were dissolved in 100 ml of dry ether, 21 g (137 mmol) of $POCl_3$ being added with stirring at ice-bath temperature. The mixture was then stirred for 3 h at room temperature and precipitates were removed. The solvent was evaporated and the residual white solid was recrystallized from acetonitrile: yield 15 g, mp<30 °C. The acid chloride obtained and 21.5 g (155 mmol) of *p*-nitrophenol were dissolved in 100 ml of dry ether, 15.5 g (155 mmol) of triethylamine being added dropwise with stirring at ice-bath temperature. After stirring for one day at room temperature, precipitates were removed and the solution was concentrated to give a waxy product. Recrystallization twice from acetone and methanol gave colorless needles of C_{18}-BNPP: yield 3 g (13%), mp 59—60 °C. The NMR spectrum was consistent with the expected structure. Found: C, 60.80; H, 7.68; N, 4.89%. Calcd for $C_{10}H_{45}N_2O_8P$: C, 60.79; H, 7.65; N, 4.83%.

Other Materials. Commercial CTAB was recrystallized twice from ethanol. Dialkyldimethylammonium bromides ($2C_nN^+2C_1$) were prepared by stepwise alkylation.[3,9]

Kinetics. Hydrolysis was initiated by injecting substrate solutions (in ethanol or acetonitrile) into aqueous solutions of surfactants containing given amounts of catalyst. The progress of the reaction was followed by the appearance of *p*-nitrophenolate anion (λ_{max}=400 nm in CTAB micelles and 390 nm in ammonium membranes, ε=18100) with a Hitachi 124 spectrophotometer. The surfactant concentration was 1×10^{-3} M (1 M=1 mol dm^{-3}), which is larger than the cmc of CTAB and $2C_nN^+2C_1$. The reaction conditions were 3 v/v% organic solvent–H_2O, μ=0.01 (KCl), 0.01—0.02 M borate buffer (pH 7—10), unless stated otherwise. The pH measurement was carried out with a Toa Digital pH meter (Type HM-10A), the pH variation of the reaction medium being smaller than 0.05.

Results

Course of Phosphoric Ester Cleavage. Ethyl bis(*p*-nitrophenyl) phosphate (C_2-BNPP) undergoes slow hydrolysis in alkaline CTAB solutions (pH 8—10). The UV absorption of C_2-BNPP (λ_{max}=270 nm) diminishes with time, new absorptions appearing at 400 and 290 nm (Fig. 1). The 400-nm band is attributable to *p*-nitrophenolate anion, one equivalent of which is formed eventually. The 290-nm band is ascribable to ethyl *p*-nitrophenyl phosphate anion (ε=9500)(C_2-MNPP$^-$) which is stable under these conditions. Tagaki *et al.*[19] confirmed that phenyl *p*-nitrophenyl phosphate anion is hydrolyzed very slowly even at 55 °C, pH 12.5. Brass and Bender[16] similarly observed the formation of *p*-nitrophenyl methylphosphonate anion at 288 nm (ε=9560) in the alkaline hydrolysis of bis(*p*-nitrophenyl) methylphosphonate.

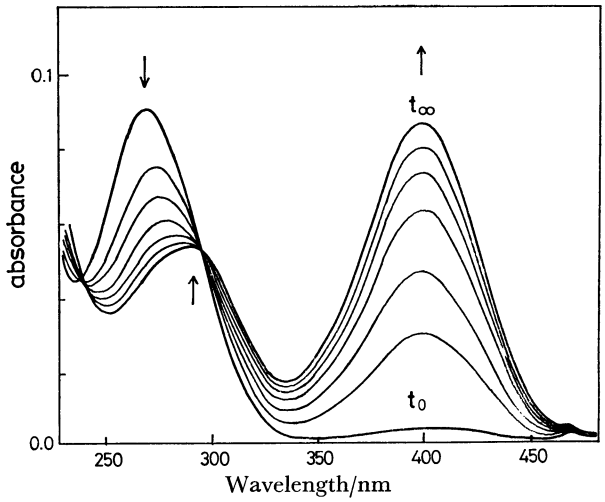

Fig. 1. Spontaneous hydrolysis of C_2-BNPP in the CTAB micelle.
pH 9.6, 30 °C, 0.01 M borate buffer, μ=0.01(KCl), 3 v/v%EtOH–H_2O. [CTAB]=1.00×10^{-3} M, [C_2-BNPP]=5.00×10^{-6} M.

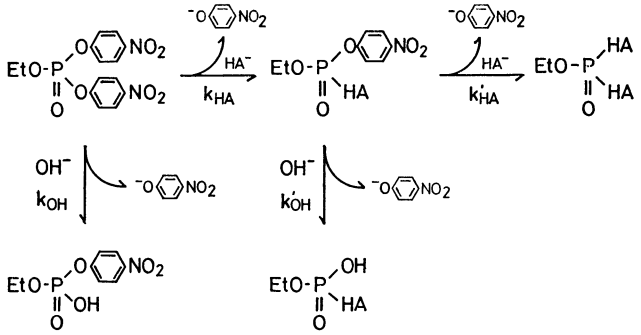

Fig. 2. The course of the ester cleavage of C_2-BNPP.

In the presence of excess hydroxamate nucleophiles, the predominant course of reaction is the release of two equivalents of *p*-nitrophenol without formation of ethyl *p*-nitrophenyl phosphate anion.

The courses of the phosphoric ester cleavage are summarized in Fig. 2. The alkaline hydrolysis (k_{OH} process) is negligible in the presence of excess of most hydroxamates, since the UV peak (λ_{max} 290 nm) characteristic of diester product C_2-MNPP$^-$ (Fig. 1) cannot be detected in the reaction mixture.

On the other hand, if equimolar amounts of substrate and nucleophile (C_{18}-MHA) are present, we observe, upon correction for the alkaline hydrolysis, rapid formation of one equivalent of *p*-nitrophenol followed by much slower *p*-nitrophenol release. These steps correspond to the k_{HA} and k'_{OH} processes (Fig. 2). Introduction of additional C_{18}-MHA during the second stage induces rapid *p*-nitrophenol release of the k'_{HA} process.

Behavior of Different Hydroxamate Nucleophiles toward C_2-BNPP. Figure 3 shows the time course of

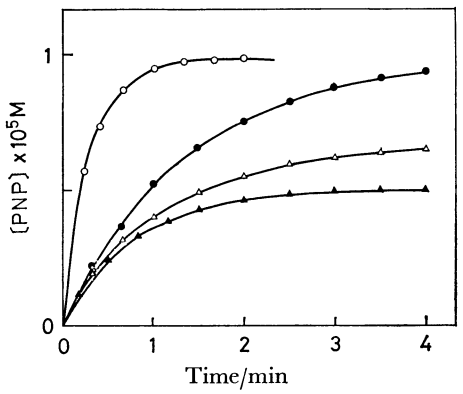

Fig. 3. The time course of the *p*-nitrophenol (PNP) release from C_2-BNPP by several hydroxamates in the presence of the CTAB micelle.
30 °C, pH 8.8, 0.02 M borate buffer, μ=0.01 (KCl), [CTAB]=1.00×10^{-3} M, [hydroxamate]=5.00×10^{-5} M, [C_2-BNPP]=5.00×10^{-6} M. *p*-Nitrophenolate anion: λ_{max} 400 nm, $\varepsilon=1.81\times10^4$. C_{18}-MHA: —○—, C_{18}-HA: —●—, C_{18}-PHA: —△—, $C_{12}N^+C_2$-MHA: —▲—.

p-nitrophenol release from C_2-BNPP by a series of long-chain hydroxamate nucleophiles in the CTAB micelle.

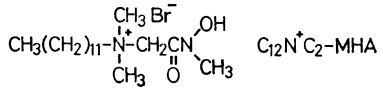

The ultimate *p*-nitrophenol release varies considerably with nucleophile. Excess of C_{18}-HA, C_{18}-MHA, and $2C_{18}$-MHA (not shown in Fig. 3) releases two equivalents of *p*-nitrophenol due to k_{HA} and k'_{HA} processes of Fig. 2. However, C_{18}-PHA produces 1.4—1.6 equivalents, the release by $C_{12}N^+C_2$-MHA being one equivalent. In the reaction with C_{18}-PHA, the difference spectrum indicates increases in absorbance at 245 and 300 nm (shoulder). The 245-nm absorption can be attributed to the monosubstitution product, the shoulder at 300 nm suggesting the formation of C_2-MNPP$^-$ (λ_{max} 290 nm, see above). The simple alkaline hydrolysis is too slow to explain the results. General base catalysis (Eq. 1) might become com-

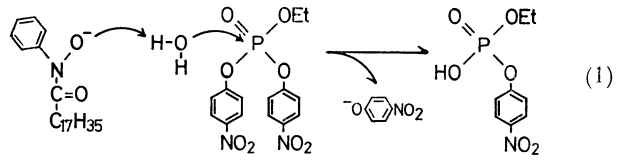

(1)

petitive with the nucleophilic process, since the latter process is rendered less efficient due to steric hindrance of the phenyl substituent near the nucleophilic center. Similarly, less than two equivalents of *p*-nitrophenol were released with related nucleophiles, BBHA and C_{12}-BHA. The release of one equivalent of *p*-ni-

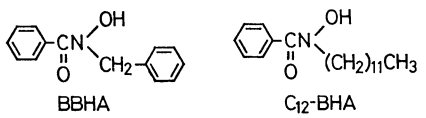

Table 1. Values of k_1 for *p*-nitrophenol release from C_2-BNPP with hydroxamate nucleophiles

Nucleophile	$10^3 k_1/s^{-1}$		
	CTAB	$2C_{12}N^+2C_1$	$2C_{16}N^+2C_1$
None(OH^-)	1.0	1.8	1.4
C_{18}-HA	9.1	35	28
C_{18}-MHA	88	100	74
C_{18}-PHA	8.3	45	50
$2C_{18}$-MHA	45	40	28

30 °C, pH 8.8, 0.02 M borate buffer, μ=0.01(KCl), [Ammonium]=1.00×10^{-3} M, [hydroxamate]=5.00×10^{-5} M, [C_2-BNPP]=5.00×10^{-6} M.

trophenol by $C_{12}N^+C_2$-MHA is ascribed to the very low reactivity of the first substitution product **1** in the subsequent nucleophilic attack. There is no indication of the general base catalysis (formation of C_2-MNPP$^-$) in this case.

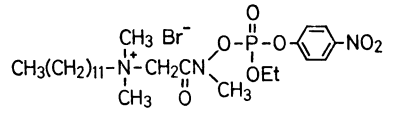

1

The presence of the $C_{12}N^+C_2$-MHA moiety in the intermediate and/or nucleophile appears to interfere with the second nucleophilic attack. This presumption is supported by the following experiments: (a) no *p*-nitrophenol release was observed when C_{18}-MHA was added to an equimolar reaction mixture (1:1 adduct formed) of C_2-BNPP and $C_{12}N^+C_2$-MHA, (b) addition of $C_{12}N^+C_2$-MHA did not promote *p*-nitrophenol release from an equimolar reaction mixture (1:1 adduct formed) of C_{18}-MHA and C_2-BNPP.

In spite of the varying extent of *p*-nitrophenol release, all the time courses of Fig. 3 obeyed the pseudo first-order kinetics (Eq. 2) for up to 80% conversion.

$$k\cdot t = -\ln\frac{A_\infty - A_t}{A_\infty}, \qquad (2)$$

where A_∞ and A_t are absorbances at the infinite time and at time t, respectively. The results indicate that the second nucleophilic attack is not slower than the first one ($k_{HA}\leqq k'_{HA}$) in the two-step nucleophilic attack toward C_2-BNPP, except in the case of $C_{12}N^+$-C_2-MHA.

The kinetic pattern of the C_2-BNPP cleavage was the same in the CTAB micelle as well as in the dialkylammonium membrane for given nucleophiles. The pseudo first-order rate constants with various hydroxamates in micellar and membrane systems are summarized in Table 1. The effective nucleophile is the hydroxamate anion. The true nucleophilic reactivity of the anion cannot be compared, since the pK_a value and consequently the fraction of the dissociated species was not determined.

Cleavage of C_{18}-BNPP. The reaction scheme for the cleavage of long-chain substrate C_{18}-BNPP is fundamentally the same as that for C_2-BNPP (Fig. 2). However, the kinetic patterns are quite different. In the reaction with excess C_{18}-HA, the first-order

kinetics holds only approximately, two equivalents of *p*-nitrophenol being released. The reaction with C_{18}-PHA was very slow ($k_{HA} \ll k_{OH}$), no further kinetic examination being performed.

In the reaction with excess C_{18}-MHA, the first-order plots in the CTAB micelle consist of two lines (Fig. 4). Since the ultimate *p*-nitrophenol release is two equivalents per mole of C_{18}-BNPP, the result

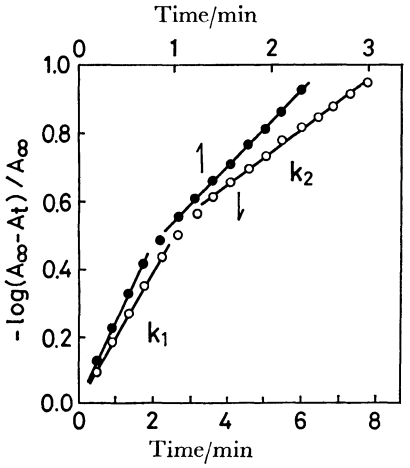

Fig. 4. Pseudo first order plots of the reaction of C_{18}-BNPP with C_{18}-MHA in the presence of the CTAB micelle.
pH 8.7, 0.02 M borate buffer, μ=0.01 (KCl), [CTAB] = 1.00×10^{-3} M, [C_{18}-MHA] = 1.00×10^{-4} M, [C_{18}-BNPP] = 1.00×10^{-5} M. 30 °C: —○—, 43 °C: —●—.

indicates that the second stage of the nucleophilic displacement (k'_{HA} process) is appreciably slower than the first stage (k_{HA} process). Similar kinetic results were obtained in the membrane system. Figure 5a shows the first order plots obtained at 30 °C. The slopes for the initial release do not vary much with the membrane. On the other hand, the slope for the second stage is suppressed increasingly with increasing lengths of the alkyl chain of the membrane. At a higher reaction temperature of 43 °C, the changes in slope are smaller except for the $2C_{18}N^+2C_1$ membrane (Fig. 5b). The apparent rate constants of the first and second steps of the reaction, k_1 and k_2, respectively, are given in Table 2. The k_1 value was determined from the initial linear portion of the first-order plots, k_2 being obtained from the second linear portions corresponding to 60—90% conversion. These two steps approximately correspond to the k_{HA} and k'_{HA} processes. The k_1 value is $(7.8\pm1.0)\times10^{-3}$

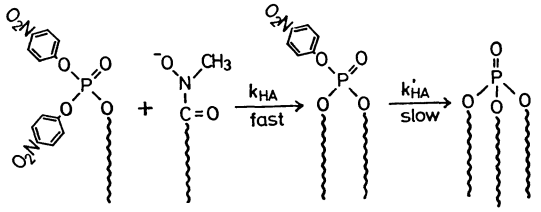

(3)

s^{-1} at 30 °C and $(18\pm3)\times10^{-3}$ s^{-1} at 43 °C, indicating that the magnitude of k_1 is not influenced by the membrane (or micelle) used.[24] In contrast, k_2 is dependent

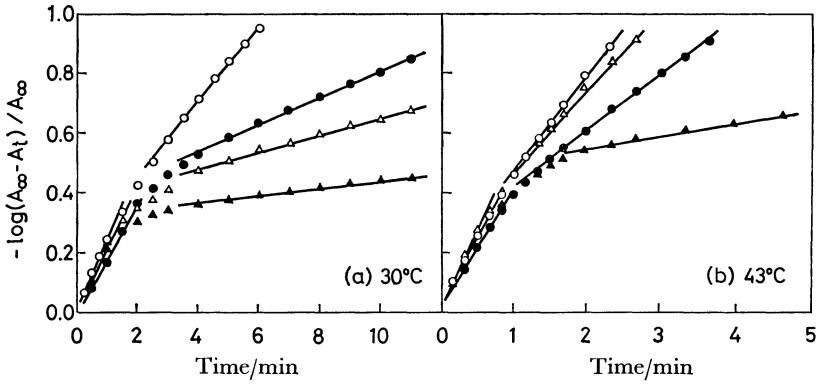

Fig. 5. Pseudo first-order plots of the reaction of C_{18}-BNPP with C_{18}-MHA in the presence of dialkylammonium membranes.
pH 8.7, 0.02 M borate buffer, μ=0.01(KCl), [C_{18}-BNPP] = 1.00×10^{-5} M, [C_{18}-MHA] = 1.00×10^{-4} M, [$2C_nN^+2C_1$] = 1.00×10^{-3} M. $2C_{12}N^+2C_1$: —○—, $2C_{14}N^+2C_1$: —●—, $2C_{16}N^+2C_1$: —△—, $2C_{18}N^+2C_1$: —▲—.

Table 2. Values of k_1, k_2, and k_2/k_1 in the reaction of C_{18}-BNPP with C_{18}-MHA

Micelle and membrane	At 30 °C			At 43 °C		
	$10^3 k_1/s^{-1}$	$10^3 k_2/s^{-1}$	k_2/k_1	$10^3 k_1/s^{-1}$	$10^3 k_2/s^{-1}$	k_2/k_1
CTAB	7.8	2.3	1/3.4	16	5.1	1/3.0
$2C_{12}N^+2C_1$	8.8	4.5	1/2.0	17	9.9	1/1.7
$2C_{14}N^+2C_1$	6.9	1.7	1/4.1	15	6.8	1/2.2
$2C_{16}N^+2C_1$	8.6	1.0	1/8.6	21	9.8	1/2.2
$2C_{18}N^+2C_1$	8.3	0.52	1/15.8	20	1.4	1/13.8

pH 8.7 (30 °C), pH 8.8 (43 °C), 0.02 M borate buffer (μ=0.01), [Ammonium] = 1.00×10^{-3} M, [C_{18}-MHA] = 1.00×10^{-4} M, [C_{18}-BNPP] = 1.00×10^{-5} M.

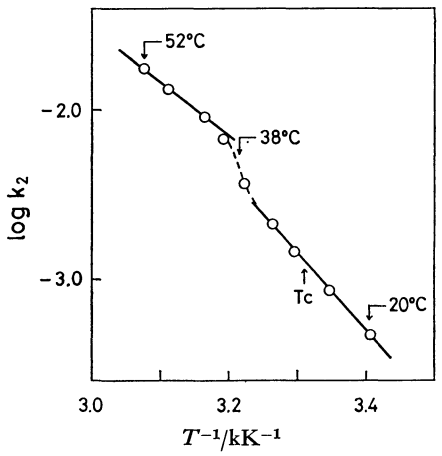

Fig. 6. Arrhenius plots for $k_{2,obsd}$ for the reaction of C_{18}-BNPP with C_{18}-MHA in the $2C_{16}N^+2C_1$ membrane.
pH 9.4, 0.02 M borate buffer, $\mu=0.01$(KCl), $[2C_{16}N^+2C_1]=1.00\times10^{-3}$ M, $[C_{18}$-MHA$]=1.00\times10^{-4}$ M, $[C_{18}$-BNPP$]=1.00\times10^{-5}$ M.

of the ammonium membrane used, decreasing with increasing alkyl chain lengths of the dialkylammonium membrane at 30 °C but not necessarily at 43 °C. A smaller k_2 value was obtained only for the $2C_{18}N^+2C_1$ membrane at higher temperature. The rate depressing effect for k_2 can be seen more clearly by comparing the ratio of the rate constants k_2/k_1. The ratio is *ca.* 1/3 for the CTAB system at both temperatures, the temperature effect being similarly small for the $2C_{12}N^+2C_1$ system. It is smaller at 30 °C than at 43 °C for the $2C_{14}N^+2C_1$ and $2C_{16}N^+2C_1$ systems, but small and constant at the two temperatures for the $2C_{18}N^+2C_1$ membrane. Since the change in k_2/k_1 due to temperature is the largest for the $2C_{16}N^+2C_1$ system, the temperature effect was studied carefully in this system. Figure 6 shows the Arrhenius plots for k_2. The plots are represented by two lines with inflection at 35 to 40 °C.

Discussion

The kinetic behavior of the nucleophilic attack of a series of long-chain hydroxamates toward phosphoric esters is summarized in Table 3. Clean second-order kinetics was observed for all the hydroxamates in the case of C_2-BNPP. This indicates that the first substitution is not faster than the second: $k_{HA}\leqq k'_{HA}$ in Fig. 1. A C_{18} alkyl chain is introduced in the first substitution. The resulting monosubstitution product is hydrophobic and the second substitution would be accelerated more efficiently in the micelles and membranes. Micellar acceleration is greater with hydrophobic substrates.

In sharp contrast with C_2-BNPP, no clean second-order kinetics could be found for C_{18}-BNPP. It appears that the steric constraint considerably retards the reaction with C_{18}-PHA and $2C_{18}$-MHA. The monosubstitution products of C_{18}-BNPP possess structures **2** and **3**. The CPK molecular model shows that the steric interference due to *N*-substituents (R)

Table 3. Kinetic behavior of various combinations of nucleophile and substrate

Nucleophile	Substrate: C_2-BNPP	Substrate: C_{18}-BNPP
C_{18}-HA	Clean second order: $k_{HA}\ll k'_{HA}$. 2 equiv. PNP released.	Approximate pseudo first order: $k_1\leqq k_2$. 2 equiv. PNP released.
C_{18}-MHA	Clean second order: $k_{HA}\ll k'_{HA}$. 2 equiv. PNP released.	Two steps in the first order plots: $k_1>k_2$. Membrane fluidity influential. 2 equiv. PNP released.
C_{18}-PHA	Clean second order: 1.4—1.6 equiv. PNP released.	PNP release very slow.
$2C_{18}$-MHA	Clean second order: $k_{HA}\ll k'_{HA}$. 2 equiv. PNP released.	Two steps in the first order plots: $k_1\gg k_2$. k_2 very small. More than equiv. PNP released.

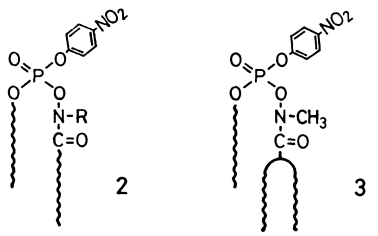

is appreciable in **2**. Thus, when R=H, mono- and disubstitutions proceed smoothly, but when R=phenyl, even the monosubstitution virtually does not proceed. When R=methyl, the monosubstitution is smooth but the disubstitution is slower. When the attacking nucleophile is a double-chain compound, even the monosubstitution is extremely slow with a *N*-methylhydroxamate ($2C_{18}$-MHA). Disubstitution proceeds faster than monosubstitution for the combination of C_2-BNPP and $2C_{18}$-MHA (Eq. 4). The double alkyl chain in $2C_{18}$-MHA may be not very demanding sterically since the double chain is removed from the phosphorus center.

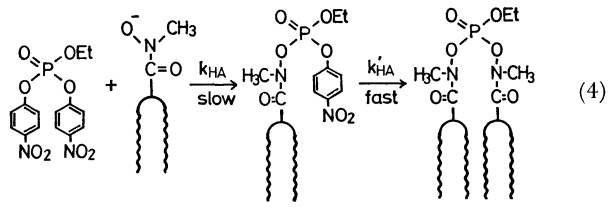

(4)

The rate constant for the pair of C_{18}-BNPP and C_{18}-MHA shows a characteristic variation with the membrane matrix. k_2 (*i.e.*, k'_{HA}) appears to be sensitive to membrane fluidity (Table 2).

The phase transition temperature (T_c) of the dialkylammonium bilayer membrane has been determined by various physicochemical means. The results determined by differential scanning calorimetry

Table 4. Phase transition temperature of dialkylammonium($2C_nN^+2C_1Br^-$) membranes

n	12	14	16	18
T_c °C	0—5	18	28	45

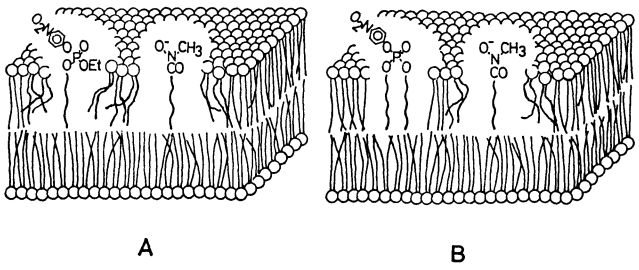

A B

Fig. 7. Schematic illustration of nucleophiles and substrates in the membrane matrix.
Note that the double-chain substrate in B perturbs the neighboring membrane less than the single-chain substrate in A.

seems to be most reliable. The T_c data are given in Table 4. At reaction temperature 30 °C, the $2C_{16}N^+2C_1$ and $2C_{18}N^+2C_1$ membranes are in the crystalline phase, their k_2 values being smaller than those in the other membranes. At reaction temperature 43 °C, only the $2C_{18}N^+2C_1$ membrane is in the crystalline state, giving a small k_2 value. The influence of the membrane fluidity is more apparent when k_2/k_1 values are compared. The membranes in the liquid crystalline state (above T_c) give k_2/k_1 ratios of 1/2—1/4, but the rigid membranes at temperatures below T_c give smaller ratios.

It may be asked why the k'_{HA} process and not the k_{HA} process is affected by membrane fluidity. The k_{HA} process is a reaction between a single-chain nucleophile and a single-chain substrate. The same type of reaction between a single-chain imidazole and a single-chain phenyl ester is influenced by phase transition.[10] The presence or absence of the influence of the membrane fluidity might depend on particular combinations of the single-chain reagents.

The k'_{HA} process is a reaction between a single-chain nucleophile and a double-chain monosubstitution product. Since the reactivity of the nucleophile (C_{18}-MHA) is not affected by membrane fluidity (k_{HA} invariant), the dependence of k'_{HA} on the membrane fluidity should arise from the varying reactivity of the double-chain intermediate. If we assume that the double-chain compound does not destroy the neighboring dialkylammonium membrane matrix, its reactivity would be affected by membrane fluidity more than the reactivity of the single-chain substrate. That is, the dialkyl species can be a part of the membrane matrix but the single-chain species should act as an impurity for the membrane. The situation is illustrated in Fig. 7.

The inflection of the Arrhenius plots (Fig. 5) is similarly associated with the phase transition, although the inflecting temperature region centered at 38 °C is 10 °C higher than T_c of the $2C_{16}N^+2C_1$ membrane (28 °C).

Table 5. Activation energy in $2C_{16}N^+2C_1$ membrane

Reaction	E_a/kcal mol^{-1} Below T_c	E_a/kcal mol^{-1} Above T_c	Remark
Nucleophilic displacement (k_{HA}' process)	21	14	This study
Decarboxylation (Eq. 5)	25	19	Ref. 12
Proton abstraction (Eq. 6)	46	20	Ref. 11

The presence of two sets of the activation energy in the membrane system has been detected in the cleavage of a phenyl ester,[10] in decarboxylation (Eq. 5),[12] and in the proton abstraction (Eq. 6).[11]

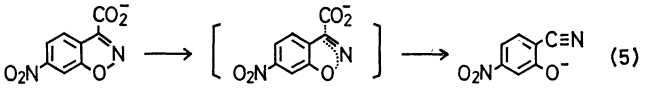

(5)

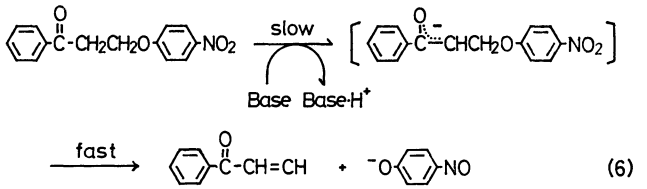

(6)

The E_a value determined from Fig. 6 is 14 kcal/mol at temperatures above T_c and 21 kcal/mol at temperatures below T_c. E_a values obtained in the temperature ranges above and below T_c for different types of reaction are compared in Table 5. In all cases, E_a below T_c is appreciably larger than E_a above T_c. It becomes more difficult for these reactions to proceed at low temperatures due to increased rigidity of the $2C_{16}N^+2C_1$ membrane matrix.

Conclusion

Phase transition is associated with the regulation of physiological functions of the biomembrane. For example, the activity of succinic acid oxidase of sheep liver mitochondria membrane changes with phase transition, the activation energy being 2 and 12 kcal/mol at temperatures above and below T_c, respectively.[25] These biochemical results are very similar to those observed for some common organic reactions: nucleophilic displacement, base-catalyzed proton abstraction, and unimolecular decarboxylation (Table 5). It is presumed that the regulation of the reaction rate by phase transition becomes possible for a large variety of organic reactions.

This study was supported in part by Grant-in-Aid for Scientific Research No. 447079 from Ministry of Education, Science and Culture.

References

1) Contribution No. 610 from the Department of Organic Synthesis.
2) T. Kunitake and Y. Okahata, *J. Am. Chem. Soc.*, **99**,

3860 (1977).
3) T. Kunitake, Y. Okahata, K. Tamaki, F. Kumamaru, and M. Takayanagi, *Chem. Lett.*, **1977**, 387.
4) T. Kajiyama, A. Kumano, M. Takayanagi, Y. Okahata, and T. Kunitake, *Chem. Lett.*, **1979**, 645.
5) Y. Okahata, R. Ando, and T. Kunitake, *Ber. Bunsenges Phys. Chem.*, in press.
6) T. Nagamura, S. Mihara, Y. Okahata, T. Kunitake, and T. Matsuo, *Ber. Bunsenges. Phys. Chem.*, **82**, 1093 (1978).
7) K. Kano, A. Romero, B. Djermouni, H. J. Ache, and J. H. Fendler, *J. Am. Chem. Soc.*, **101**, 4030 (1979).
8) T. Kunitake and T. Sakamoto, *J. Am. Chem. Soc.*, **100**, 4615 (1978).
9) Y. Okahata, R. Ando, and T. Kunitake, *Bull. Chem. Soc. Jpn.*, **52**, 3647 (1979).
10) T. Kunitake and T. Sakamoto, *Chem. Lett.*, **1979**, 1059.
11) Y. Okahata, S. Tanamachi, and T. Kunitake, *Nippon Kagaku Kaishi*, **1980**, 442.
12) T. Kunitake, Y. Okahata, R. Ando, S. Shinkai, and S. Hirakawa, *J. Am. Chem. Soc.*, **102**, 7877 (1980).
13) Earlier examples of the use of micellar hydroxamate nucleophiles toward carboxylic acid esters include I. Tabushi, Y. Kuroda, and S. Kita, *Tetrahedron Lett.*, **1974**, 643; I. Tabushi, and Y. Kuroda, *ibid.*, **1974**, 3613; T. Kunitake, Y. Okahata, and T. Sakamoto, *Chem. Lett.*, **1975**, 459.
14) S. A. Khan and A. J. Kirby, *J. Chem. Soc., B*, **1970**, 1172.
15) A. Williams and R. A. Naylon, *J. Chem. Soc., B*, **1971**, 1967.
16) H. J. Brass and M. L. Bender, *J. Am. Chem. Soc.*, **94**, 7421 (1972).
17) C. A. Bunton and Y. Ihara, *J. Org. Chem.*, **42**, 2865 (1977).
18) J. Epstein, J. J. Kaminski, N. Bodor, R. Enever, J. Sowa, and T. Higuchi, *J. Org. Chem.*, **43**, 2816 (1978).
19) W. Tagaki, T. Eiki, and H. Kaneko, The 28th Symposium on Organic Reaction Mechanisms, November 1977, Yokohama, Preprint, p. 207.
20) T. Kunitake, Y. Okahata, and T. Sakamoto, *J. Am. Chem. Soc.*, **98**, 7799 (1976).
21) T. Kunitake, Y. Okahata, and T. Tahara, *Bioorg. Chem.*, **5**, 155 (1976).
22) T. Sakamoto, unpublished synthesis in these laboratories.
23) M. Rapp, *Liebigs. Ann. Chem.*, **224**, 161 (1884).
24) The k_1 and k_2 values in the $2C_{14}N^+2C_1$ membrane are slightly smaller than expected. Small deviations from the first-order plot were observed in the initial stage of the *p*-nitrophenol release, the reaction mixture becoming turbid in some cases. These observations suggest that the reacting species are not entirely miscible with the $2C_{14}N^+2C_1$ membrane, and explain the small, negative deviations of k_1 and k_2.
25) E. J. McMurchie and J. K. Raison, *Biochim. Biophys. Acta*, **554**, 364 (1979).